DEPARTMENT OF THE INTERIOR

U.S. GEOLOGICAL SURVEY

In Situ Geomechanics of Crystalline and Sedimentary Rocks

Part VII:

SLIP--A FORTRAN computer program for computing the potential for sliding on arbitrarily oriented weakness planes in triaxial stress states

By

William Z. Savage[1] and Henri S. Swolfs[1]

Open-File Report 87-82

This report is preliminary and has not been reviewed for conformity with U.S. Geological Survey editorial standards.

[1]Golden, Colorado

1987

IN SITU GEOMECHANICS OF CRYSTALLINE AND SEDIMENTARY ROCKS

PART VII: SLIP--A FORTRAN COMPUTER PROGRAM FOR COMPUTING THE POTENTIAL FOR SLIDING ON ARBITRARILY ORIENTED WEAKNESS PLANES IN TRIAXIAL STRESS STATES

By William Z. Savage and Henri S. Swolfs

PREFACE

This report is the seventh of a series summarizing the results of the U.S. Geological Survey's research program in geomechanics aimed at investigating and assessing the potential of crystalline and sedimentary rock masses as geological repositories of nuclear waste. The first six parts of this series of reports are referenced below:

Savage, W.Z., and Swolfs, H.S., 1980, The long-term deformation and time-temperature correspondence of viscoelastic rock--an alternative theoretical approach, Pt. 1 of In situ geomechanics of crystalline and sedimentary rocks: U.S. Geological Survey Open-File Report 80-708, 21 p.

Smith, W.K., 1982, Two BASIC computer programs for the determination of in situ stresses using the CSIRO hollow inclusion stress cell and the USBM borehole deformation gage [Pt. 2 of In situ geomechanics of crystalline and sedimentary rocks]: U.S. Geological Survey Open-File Report 82-489, 40 p.

Swolfs, H.S., 1982, First experiences with the C.S.I.R.O. hollow-inclusion stress cell, Pt. 3 of In situ geomechanics of crystalline and sedimentary rocks: U.S. Geological Survey Open-File Report 82-990, 10 p.

Nichols, T.C., Jr., 1983, Continued field testing of the modified U.S. Geological Survey 3-D borehole stress probe, Pt. 4 of In situ geomechanics of crystalline and sedimentary rocks: U.S. Geological Survey Open-File Report 83-750, 11 p.

Savage, W.Z., Powers, P.S., and Swolfs, H.S., 1984, RVT--A FORTRAN program for an exact elastic solution for tectonic and gravity stresses in isolated symmetric ridges and valleys, Pt. 5 of In situ geomechanics of crystalline and sedimentary rocks: U.S. Geological Survey Open-File Report 84-827, 12 p.

Swolfs, H.S., and Powers, P.S., 1985, An update on two BASIC computer programs for the determination of in situ stresses using the CSIRO hollow inclusion cell and the USBM borehole deformation gage, Pt. 6 of In situ geomechanics of crystalline and sedimentary rocks: U.S. Geological Survey Open-File Report 85-509, 15 p.

Published journal articles that report on the findings of this program are referenced below:

Swolfs, H.S., and Kibler, J.D., 1982, A note on the Goodman Jack: Rock Mechanics, v. 15, no. 2, p. 57-66.

Swolfs, H.S., 1983, Aspects of the size-strength relationship of unjointed rocks: Chapter 51 in Rock Mechanics--Theory-Experiment-Practice: 24th U.S. Symposium on Rock Mechanics, College Station, Texas, p. 501-510.

Swolfs, H.S., 1984, The triangular stress diagram - a graphical representation of crustal stress measurements: U.S. Geological Survey Professional Paper 1291, 19 p.

Swolfs, H.S., and Savage, W.Z., 1984, Site characterization studies of a volcanic cap rock, Chapter 39 in Rock Mechanics in Productivity and Protection: 25th U.S. Symposium on Rock Mechanics, Evanston, Illinois, p. 370-380.

Savage, W.Z., Swolfs, H.S., and Powers, P.S., 1985, Gravitational stresses in long symmetric ridges and valleys: International Journal of Rock Mechanics, Mining Sciences, and Geomechanical Abstracts, v. 22, no. 5, p. 291-302.

Swolfs, H.S., and Savage, W.Z., 1985, Topography, stresses, and stability at Yucca Mountain, Nevada, in Research & Engineering Applications in Rock Masses: 26th U.S. Symposium on Rock Mechanics, v. 2, p. 1121-1129.

Savage, W.Z., and Swolfs, H.S., 1986, Tectonic and gravitational stress in long symmetric ridges and valleys: Journal of Geophysical Research, v. 91, no. B3, p. 3677-3685.

Swolfs, H.S., and Savage, W.Z., 1986, Topographic modification of in situ stress in extensional and compressional tectonic environments: Proceedings of the International Symposium on Rock Stress and Rock Stress Measurements, Stockholm, Sweden, p. 89-98.

CONTENTS

ILLUSTRATIONS

ILLUSTRATIONS--Continued

PART VII: SLIP--A FORTRAN COMPUTER PROGRAM FOR COMPUTING THE POTENTIAL SLIDING ON ARBITRARILY ORIENTED WEAKNESS PLANES IN TRIAXIAL STRESS STATES

By
WILLIAM Z. SAVAGE AND HENRI S. SWOLFS

INTRODUCTION

The potential for sliding on planes of weakness such as faults or joints under general stress states in rocks has previously been analyzed graphically by the Mohr-circle construction (Wallace, 1951; Jaeger, 1962; and Jaeger and Cook, 1969). Because such analyses tend to be rather labor intensive, we have developed a FORTRAN computer program, SLIP, which automates this process. This program gives, in coordinates appropriate for stereographic projection, the orientations of planes on which slip can occur and the direction of slip on each plane for general triaxial stress states when all principal stresses are compressive.

In what follows, we present the theoretical background for the computer program beginning with a description of the concepts of the state of stress at a point, the Cauchy relationship between the state of stress at a point and the stress vector, and the shear and normal components of the stress vector on a plane and their directions. Also, the criterion in terms of shear and normal stress vector components for frictional slip on an arbitrary weakness plane (Amonton's Law, Jaeger and Cook, 1969), the mathematics of stereographic projection, and the uses of each in the computer program are described. Some examples of orientations of potential slip planes and slip directions calculated by the program SLIP (listed in the appendix) are shown in stereographic projection in the final section.

STATE OF STRESS AT A POINT

The state of stress at a point represented by the infinitesimal cube with nine stress components σ_{ij}, is shown in figure 1. The stress tensor is symmetric where

$\sigma_{ij} = \sigma_{ji}$,

σ_{11}, σ_{22}, σ_{33} are normal stresses, and

$\sigma_{12} = \sigma_{21}$ $\sigma_{13} = \sigma_{31}$ $\sigma_{23} = \sigma_{32}$ are shear stress components.

If σ_{11}, σ_{22}, and σ_{33} act on planes with zero shear stresses, then

σ_{11}, σ_{22}, and σ_{33} are principal stresses.

CAUCHY RELATIONSHIP

Consider the tetrahedron formed by the three coordinate axis planes and the infinitesimal plane ABC (figure 2). The plane ABC has an area ds and a normal $\vec{n}$ with direction cosines

$$\eta_1 = \cos(\vec{n},x_1),\ \eta_2 = \cos(\vec{n},x_2),\ \eta_3 = \cos(\vec{n},x_3)$$

The area of the infinitesimal surface OBC is $ds_1 = ds\cos(\vec{n},x_1) = \eta_1 ds$, the area of the infinitesimal surface OAC is $ds_2 = \eta_2 ds$, and the area of the infinitesimal surface OAB is $ds_3 = \eta_3 ds$.

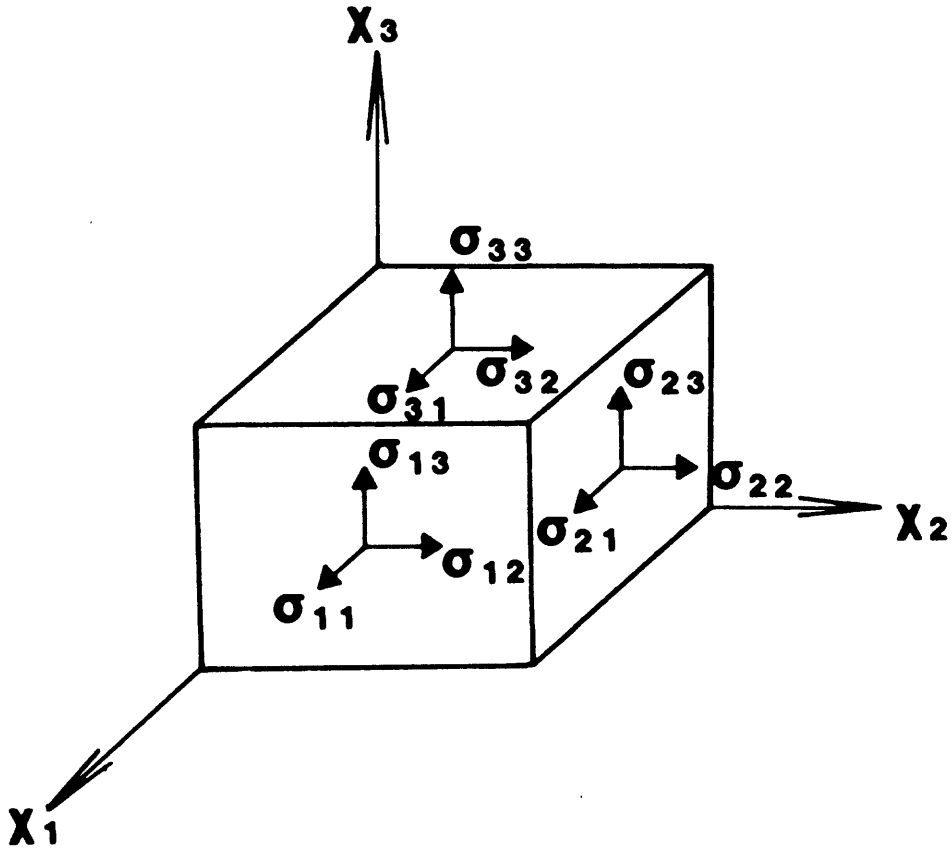

Figure 1. State of stress at a point in x_i coordinates. σ_{11}, σ_{22}, σ_{22} are the normal stress components and $\sigma_{12} = \sigma_{21}$, $\sigma_{13} = \sigma_{31}$, and $\sigma_{23} = \sigma_{32}$ are the shear stress components.

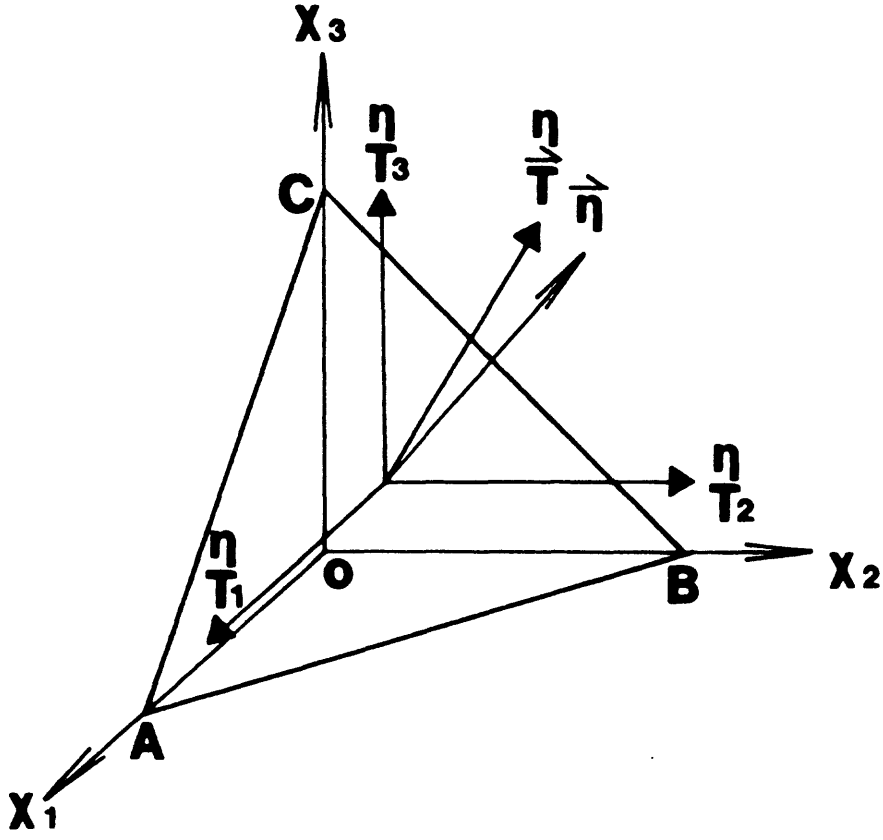

Figure 2. Stress vector $\vec{T}^{\eta}$ and components T_i^{η} acting on the infinitesimal plane ABC with normal $\vec{\eta}$.

Calling T_i^{η} the components of the stress vector $\vec{T}^{\eta}$ acting on ABC, we have for equilibium of forces in the x_1, x_2, and x_3 directions

$$T_i^{\eta} ds = ds_1 \sigma_{i1} + ds_2 \sigma_{i2} + ds_3 \sigma_{i3},$$

that is

$$T_1^{\eta} = \sigma_{11}\eta_1 + \sigma_{21}\eta_2 + \sigma_{31}\eta_3$$
$$T_2^{\eta} = \sigma_{12}\eta_1 + \sigma_{22}\eta_2 + \sigma_{32}\eta_3$$
$$T_3^{\eta} = \sigma_{13}\eta_1 + \sigma_{23}\eta_2 + \sigma_{33}\eta_3$$

or,

$$T_i^{\eta} = \sigma_{ji}\eta_j.$$

Cauchy's formula establishes the relationship between the stress tensor σ_{ij} at a point and the stress vector T_i^{η} on a plane of arbitrary orientation through that point.

SHEAR AND NORMAL COMPONENTS OF THE STRESS VECTOR ON A PLANE

By resolving $\vec{T}^{\eta}$ into components normal and tangential to the infinitesimal plane ABC (fig. 3), we find the magnitude of the normal stress component to be

$$\sigma_n = \vec{T}^{\eta} \cdot \vec{\eta} = \sigma_{ji}\eta_j\eta_i = T_i^{\eta}\eta_i$$

and the magnitude of shearing or tangential stress component is given by

$$\sigma_s^2 = R^2 - \sigma_n^2$$

where the magnitude of $\vec{T}^{\eta}$ is given by $|\vec{T}^{\eta}| = \sqrt{T_1^{\eta 2} + T_2^{\eta 2} + T_3^{\eta 2}} = R.$

If the coordinate axes x_i are chosen to be in principal stress directions, we have

$$T_1^{\eta} = \sigma_{11}\eta_1$$
$$T_2^{\eta} = \sigma_{22}\eta_2$$
$$T_3^{\eta} = \sigma_{33}\eta_3$$

and

$$\sigma_s^2 = \sigma_{11}^2\eta_1^2 + \sigma_{22}^2\eta_2^2 + \sigma_{33}^2\eta_3^2 - [\sigma_{11}\eta_1^2 + \sigma_{22}\eta_2^2 + \sigma_{33}\eta_3^2]^2$$

or

$$\sigma_s^2 = T_1^{\eta 2} + T_2^{\eta 2} + T_3^{\eta 2} - [T_1^{\eta}\eta_1 + T_2^{\eta}\eta_2 + T_3^{\eta}\eta_3]^2.$$

Note that no ordering with respect to magnitude is implied; that is, σ_{11}, σ_{22}, and σ_{33} can have arbitrary values relative to each other.

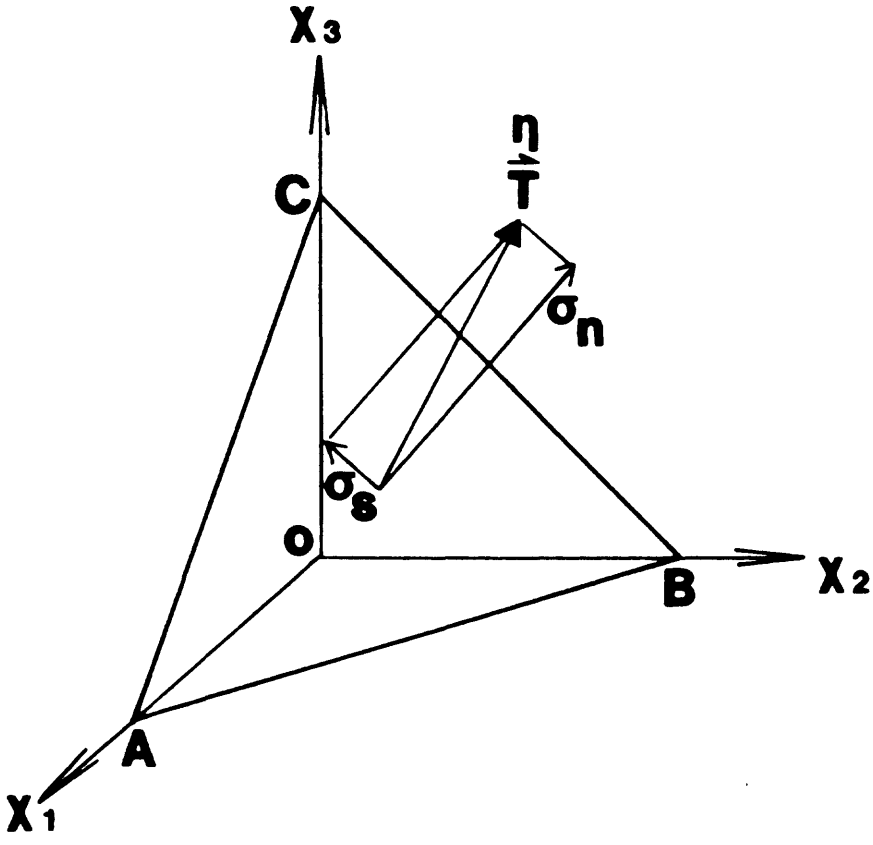

Figure 3. Stress vector $\vec{T}^{\eta}$ and components σ_s and σ_n acting on ABC.

SHEAR STRESS DIRECTIONS

The relation developed for shear stress on the plane ABC gives the magnitude of σ_s only. Some additional relations are needed to give the direction of σ_s.

The direction cosines of the normal to the plane ABC are given by η_1, η_2, and η_3 (fig. 4). Consider a vector $\vec{OS}$ normal to the plane defined by $\vec{T}$ and $\vec{\eta}$ in figure 4. Let this vector have direction cosines ν_1, ν_2, and ν_3. Now the vector $\vec{T}$ has direction ratios T_1^η, T_2^η, and T_3^η. Then by the rules of vector algebra we have

$$\nu_1 = \eta_2 T_3^\eta - \eta_3 T_2^\eta$$

$$\nu_2 = \eta_3 T_1^\eta - \eta_1 T_3^\eta$$

$$\nu_3 = \eta_1 T_2^\eta - \eta_2 T_1^\eta$$

The vector $\vec{OR}$ shown in figure 4, to which we assign direction cosines λ_1, λ_2, and λ_3, is parallel to σ_s and normal to the plane defined by OSP. Again, by the rules of vector algebra, we find

$$\lambda_1 = \eta_2[\eta_1 T_2^\eta - \eta_2 T_1^\eta] - \eta_3[\eta_3 T_1^\eta - \eta_1 T_3^\eta]$$

$$\lambda_2 = \eta_3[\eta_2 T_3^\eta - \eta_3 T_2^\eta] - \eta_1[\eta_1 T_2^\eta - \eta_2 T_1^\eta]$$

$$\lambda_3 = \eta_1[\eta_3 T_I^\eta - \eta_1 T_3^\eta] - \eta_3[\eta_2 T_3^\eta - \eta_3 T_2^\eta]$$

for the direction of σ_s.

SLIP CRITERION

Consider the plane ABC to be a plane of weakness within a rock mass across which sliding can occur if the shear stress and normal stress on that plane are uniform and satisfy the relation

$$\sigma_s = \mu\sigma_n$$

where μ is the coefficient of sliding friction. Thus, as the shear and normal stresses acting on the plane are functions of the three normal stresses σ_{11}, σ_{22}, and σ_{33}, and the plane orientation is given by the direction cosines η_1, η_2, and η_3, we can investigate those normal stress combinations and weakness plane orientations for which $\sigma_s > \mu\sigma_n$ and slip can occur. Further, assuming that slip will be in the direction of σ_s, we can calculate the slip direction using the equations for direction cosines λ_i.

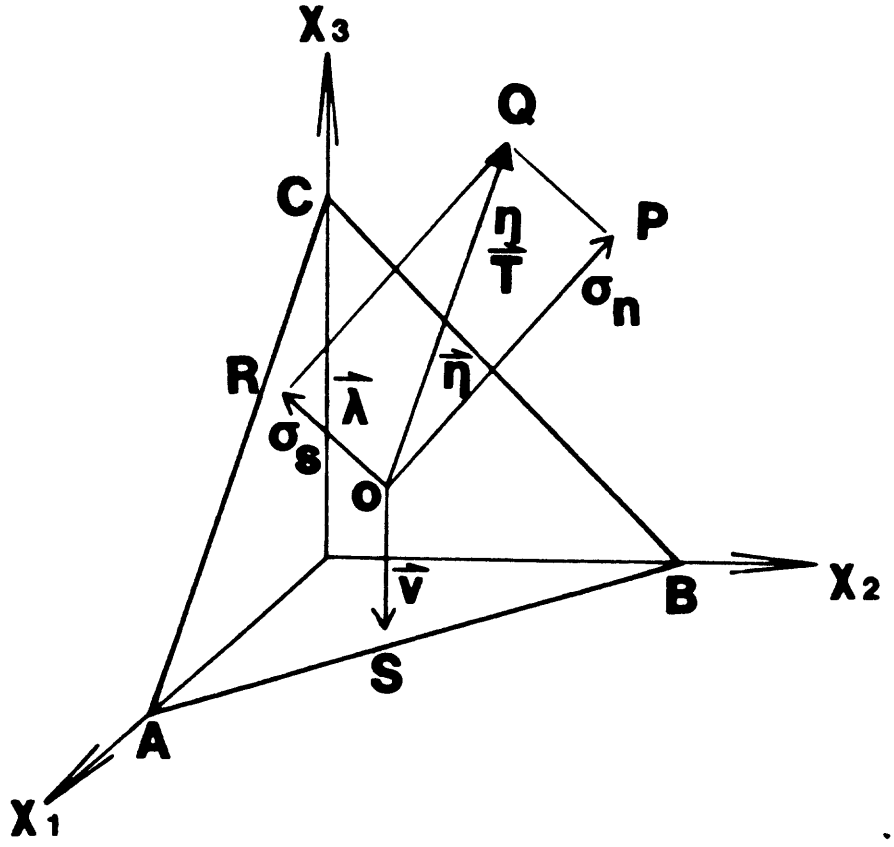

Figure 4. Vector relationships for defining the direction of the shear stress component, σ_s.

STEREOGRAPHIC PROJECTION

In order to clearly present the orientation of planes along which slip can occur and the associated slip directions for various combinations of σ_{11}, σ_{22}, and σ_{33}, we convert the cosines η_1, η_2, and η_3 to the spherical polar form shown in figure 5 where

$$\eta_1 = \sin\theta\cos\alpha$$

$$\eta_2 = \sin\theta\sin\alpha$$

$$\eta_3 = \cos\theta.$$

The calculation of stress magnitudes in given planes then proceeds by incrementing θ and α in small angles from 0 to $\pi/2$ and comparing normal and shear stresses at each point to the slip criterion. Planes across which slip can occur are then plotted in stereographic projection by the following method.

For conformal stereographic presentation, we have the following (Goodman, 1976, and figure 5):

$$OV = \tan[\theta/2]$$

and

$$x = OV\cos\alpha$$

$$y = OV\sin\alpha.$$

F is the focus of the projection. In the appended computer program, normals to planes on which slip occurs for combinations of σ_{11}, σ_{22}, σ_{33}, and μ are given in the xy coordinates appropriate for stereographic projection.

To represent the slip direction associated with each plane on which slip occurs, we calculate a new set of angles θ' and α' from

$$\theta' = \cos^{-1}\lambda_3$$

and

$$\alpha' = \tan^{-1}[\lambda_2/\lambda_1].$$

Then using the relationships

$$(OV)' = \tan[\theta'/2]$$

and

$$x' = (OV)'\cos\alpha'$$

$$y' = (OV)'\sin\alpha',$$

we can plot slip directions in stereographic projection.

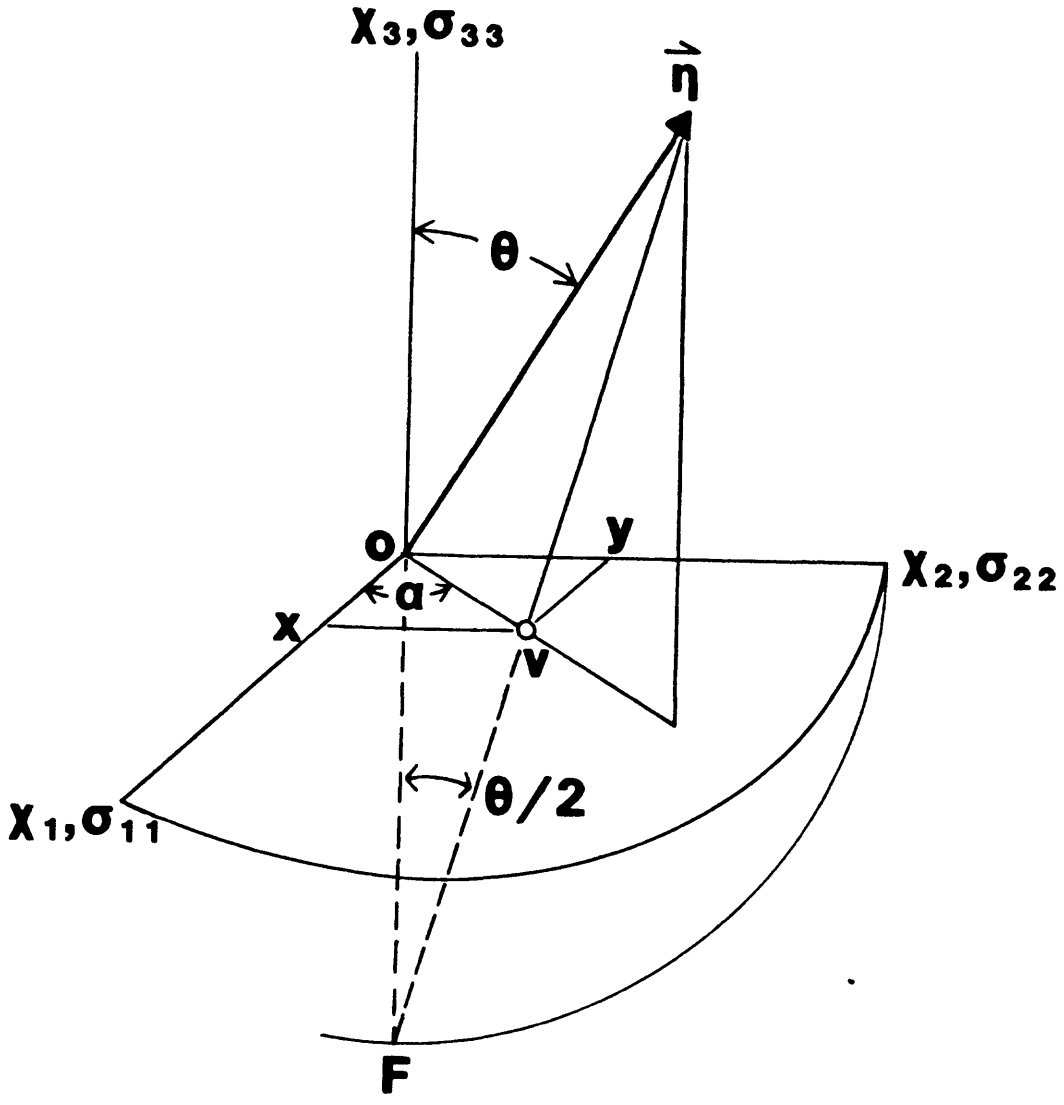

Figure 5. Spherical polar coordinates and construction for equi-angular stereographic projection.

DESCRIPTION OF SLIP.FOR

A FORTRAN-77 program listing of SLIP.FOR is given in the Appendix. This program is written for a Digital Equipment Corporation VAX-750 with VMS operating system. The only input required are the ratios $s_x = \sigma_{11}/\sigma_{22}$, $s_y = \sigma_{22}/\sigma_{22}$, $s_z = \sigma_{33}/\sigma_{22}$, and the friction coefficient μ.

Calculations of normal and shear stresses and the yield function are carried out as described in the previous section on stereographic projection. This information (in stereographic x, y coordinates) is written to the file SLIP.DAT. Normals to planes across which slip can occur and the slip directions are output in files SLIP1.DAT and SLIP2.DAT respectively. Both sets of data are in stereographic x, y coordinates and can be used with appropriate xy plotting software to produce plots of the type shown in the next section. Note that no xy plot software is included here.

EXAMPLES

We conclude with some examples calculated with SLIP.FOR. Figure 6 is a computer generated stereographic projection of poles to planes on which slip can occur for $\mu = 0.67$, and the normalized principal stresses $s_x = \sigma_{11}/\sigma_{22} = 0.1$, $s_y = \sigma_{22}/\sigma_{22} = 1.0$, and $0.1 < s_z = \sigma_{33}/\sigma_{22} < 1.0$. Figure 6 is identical to figure 3.82 on page 72 of Jaeger and Cook (1979) which was produced by a three-dimensional Mohr circle graphical analysis described in Jaeger (1962).

Figure 7 shows several panels of computer generated stereographic plots of poles to possible slip planes (p) and associated slip directions (s) for the case of thrust faulting where s_x, the intermediate stress, varies between 1.0 and 0.33, $s_y = 1.0$, s_z, the least vertical stress, equals 0.3, and $\mu = 0.6$. Note that although the orientations of all possible slip planes and associated slip directions are shown, each plane will have a unique slip direction on it given by the equations λ_1, λ_2, and λ_3. It is interesting to note the small range of slip plane orientations and slip directions for values of the intermediate principal stress (in this case s_x) between 0.6 and 0.8. The range of orientations and slip directions increases as s_x approaches either the least principal stress, s_z, or the greatest principal stress, s_y.

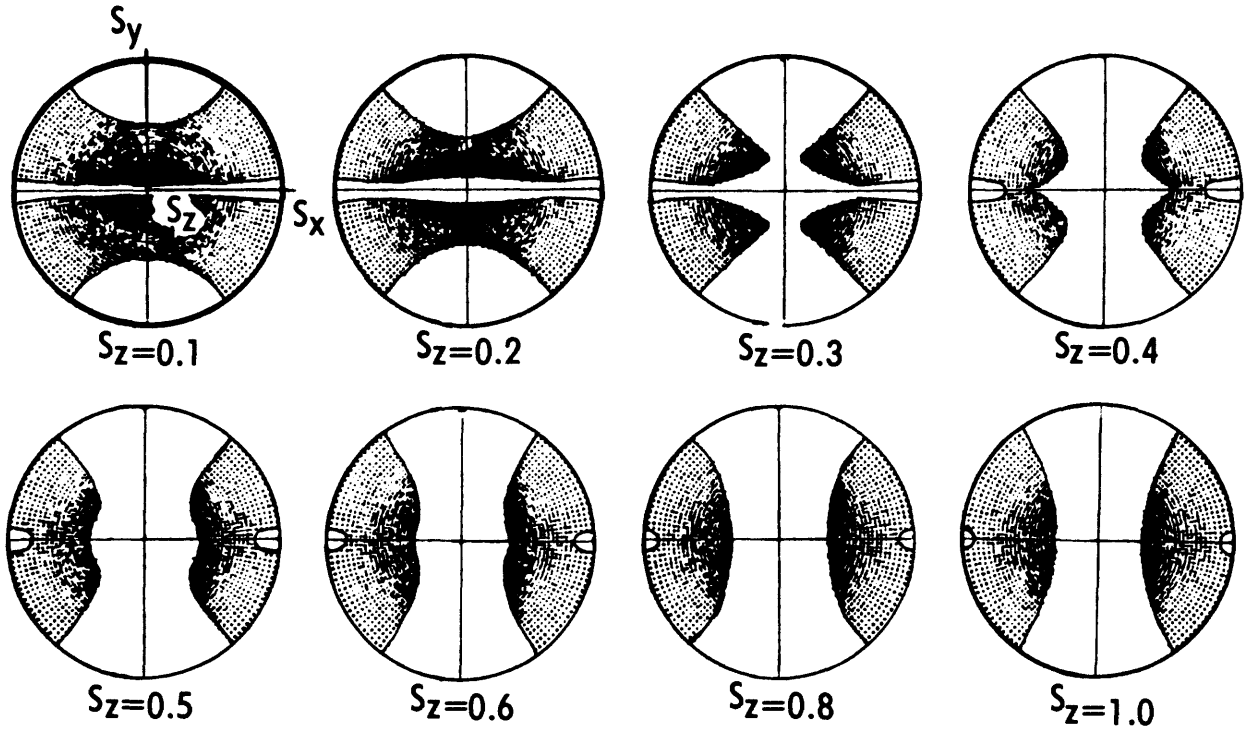

Figure 6. Stereographic projection of calculated regions (stippled) in which poles to planes of weakness must fall for slip to be possible when $\mu = 0.67$, $s_x = 0.1$, $s_y = 1.0$, and $s_z = 0.1$, 0.2, 0.3, 0.4, 0.5, 0.6, 0.8, and 1.0. Orientations of s_x, s_y, and s_z are shown in the first figure.

When s_x equals s_z, we have the situation shown in the first panel of figure 8. From here through the remaining five panels of figure 8, orientations of poles to possible slip planes and associated slip directions are shown for strike slip faulting where $\mu = 0.6$, s_x, the least principal stress, equals 0.3, s_y, the greatest principal stress, equals 1.0, and the intermediate principal stress, s_z, varies between 0.3 and 0.9. The relative ordering of s_x, s_y, and s_z in figure 8 is the same as in figure 6, but here the stress differences are smaller permitting a smaller range of potential slip planes. The range of slip plane orientations and slip directions changes rapidly when the magnitudes of s_x and s_z are close (first four panels of figure 8), becomes more restricted for values of s_z between 0.4 and 0.6, and begins to broaden again as s_z approaches s_y.

The first panel of figure 9 shows the orientations of poles to possible slip planes and associated slip directions when $s_z = s_y$. In this and the succeeding panels of figure 9, orientations of poles to possible slip planes and associated slip directions are shown for normal faulting where $\mu = 0.6$, $s_x = 0.3$, s_y varies between 1.0 and 0.3, and $s_z = 1.0$. Note again the rapid changes in orientations and directions for values of s_y close to either s_z or s_x, and the relative lack of change for intermediate values of s_y. Finally, in figure 9 and the preceding two figures (8 and 7), notice that the greatest range of possible slip plane orientations and slip directions is obtained when two of the principal stresses are equal. Also note that in each case nothing has been said about the sense of slip because this is known either through experimentation or field observations (Jaeger and Cook, 1969).

The last set of computer generated stereographic plots shows the influence of increasing the friction coefficient μ, from 0.6 to 0.8, and finally, to 0.85 for the case where $s_z = 1.0$ and $s_x = s_y = 0.2$ (figure 10a), and where $s_x = s_y = 1.0$ and $s_z = 0.2$ (figure 10b). As might be expected, the range of possible slip planes decreases as the coefficient of sliding friction is increased.

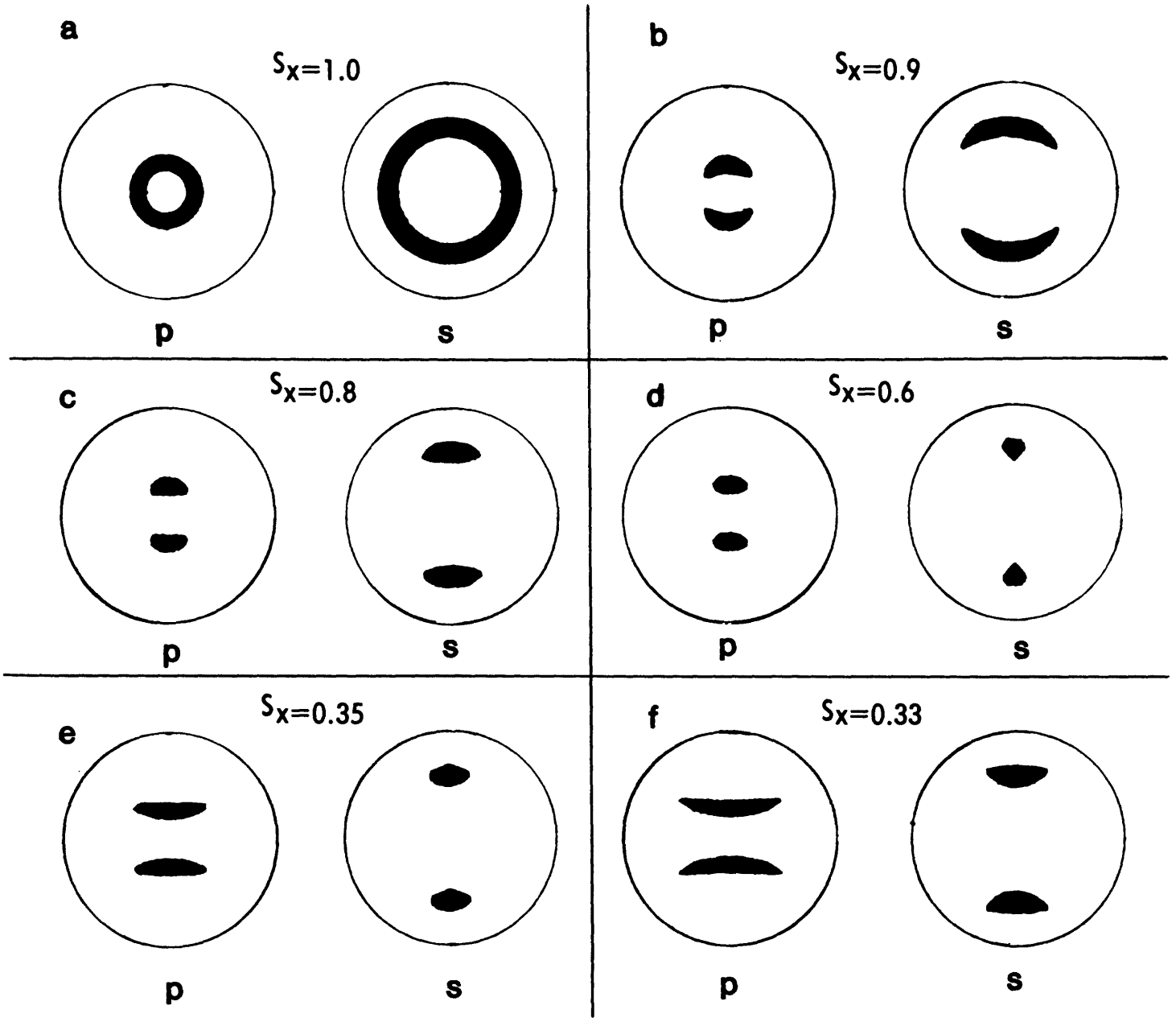

Figure 7. Orientation of poles to possible slip planes (p) and associated slip direction (s) for thrust faulting where μ=0.6, $0.33 \leq s_x \leq 1.0$, s_y=1.0, and s_z=0.3.

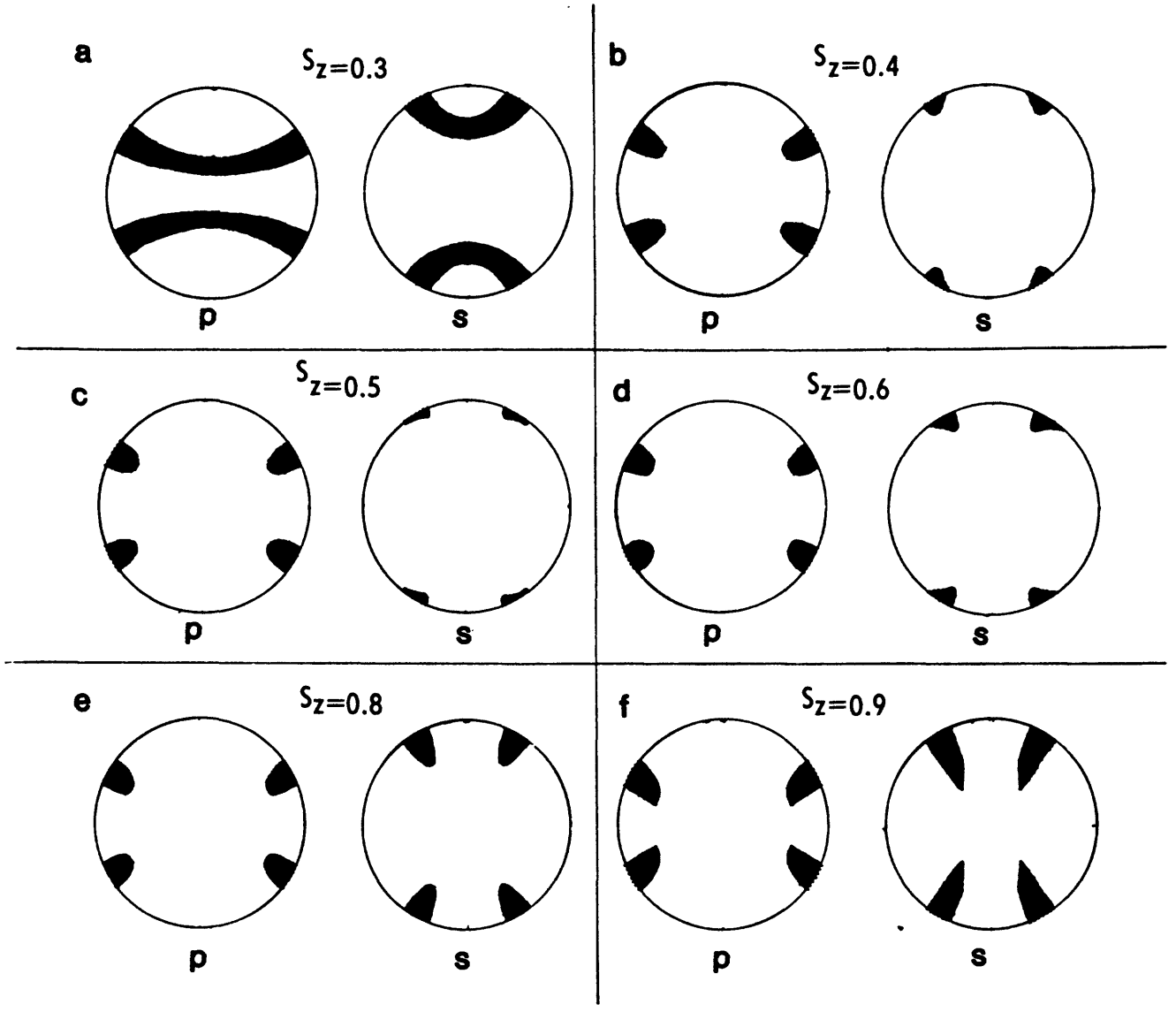

Figure 8. Orientation of poles to possible slip planes (p) and associated slip directions (s) for strike slip faulting where $\mu = 0.6$, $s_x = 0.3$, $s_y = 1.0$, and $0.3 \leqq s_z \leqq 0.9$.

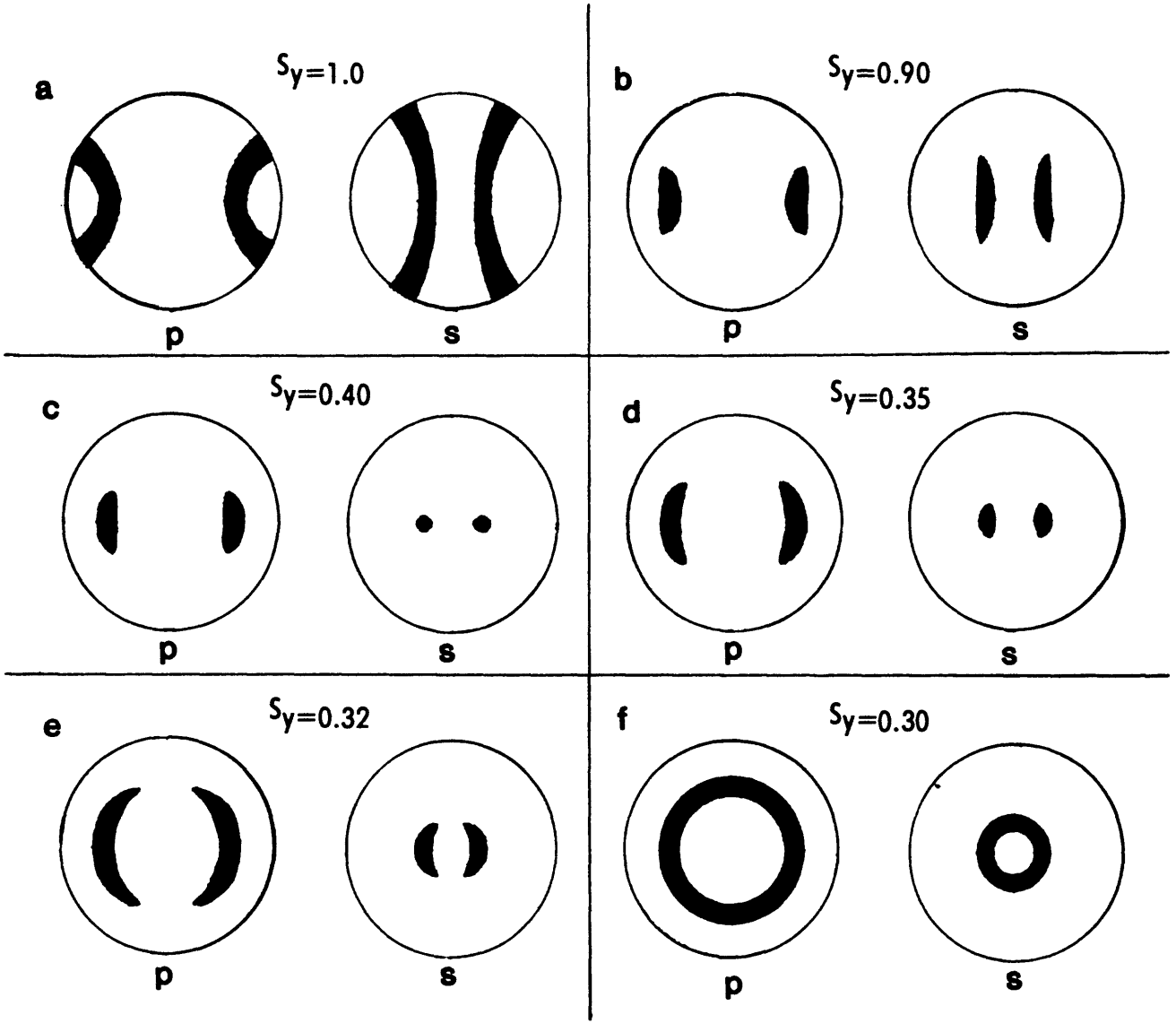

Figure 9. Orientation of poles to possible slip planes (p) and associated slip directions (s) for normal faulting where $\mu = 0.6$, $s_x = 0.3$, $0.3 \leqq s_y \leqq 1.0$, and $s_z = 1.0$.

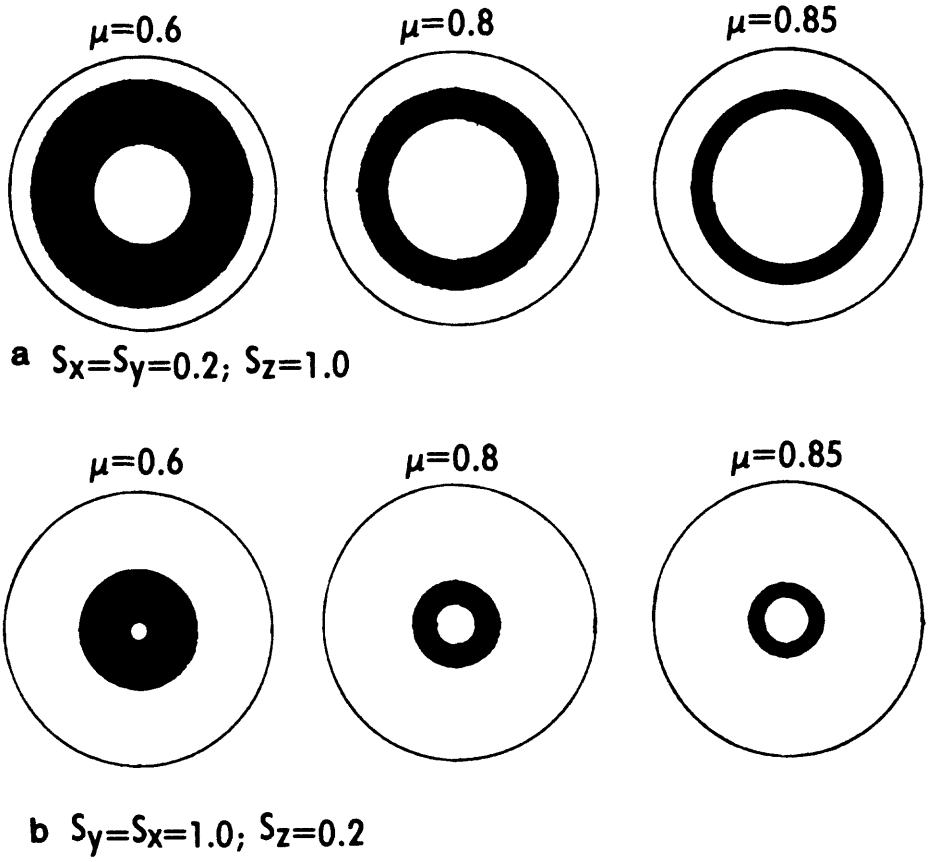

Figure 10. Distribution of poles to planes along which slip can occur for (a) s_z=1.0, s_x=s_y=0.2, (b) s_z=s_y=1.0, s_z=0.2, and increasing values of μ (0.6, 0.8, 0.85).

REFERENCES CITED

1. Goodman, R.R., 1976, Methods of Geological Engineering in Discontinuous Rocks, West Publishing Company, St. Paul, Minnesota, 472 p.

2. Jaeger, J.C., 1962, Elasticity, Fracture and Flow, 2nd ed., Methuen and Company, London, 212 p.

3. Jaeger, J.C., and Cook, N.G.W., 1969, Fundamentals of Rock Mechanics, Methuen and Company, London, 513 p.

4. Wallace, R.E., 1951, Geometry of shearing stress and relation to faulting, Journal of Geology, v. 55, no. 2, p. 118-130.

APPENDIX

SLIP.FOR

```
      open(30,file='slip.dat',form='formatted',status='new')
      open(31,file='slipl.dat',form='formatted',status='new')
      open(32,file='slip2.dat',form='formatted',status='new')
      rad=.01745
      tinc=2.5
      tint=0.0
      tfin=90.0
      ainc=2.5
      aint=0.0
      afin=90.0
      print *, 'Enter sigx,sigy,sigz,emu'
      read *,sigx,sigy,sigz,emu
      write(30,6)sigx,sigy,sigz,emu
      write(31,6)sigx,sigy,sigz,emu
      write(32,6)sigx,sigy,sigz,emu
      theta=aint*rad
1     alfa=aint*rad
2     el=sin(theta)*cos(alfa)
      e2=sin(theta)*sin(alfa)
      e3=cos(theta)
      px=el*sigx
      py=e2*sigy
      pz=e3*sigz
      rsq=px**2+py**2+pz**2
      sgn2=(el*px+e2*py+e3*pz)**2
      tsq=rsq-sgn2
      f=tsq-sgn2*emu**2
      sigs=sqrt(abs(rsq-sgn2))
      sign=sqrt(sgn2)
      tau=f
      ov=tan(.5*theta)
      x=ov*cos(alfa)
      y=ov*sin(alfa)
      if(tau.lt.0.0) go to 5
      al=e2*(el*py-e2*px)-e3*(e3*px-el*pz)
      a2=e3*(e2*pz-e3*py)-el*(el*py-e2*px)
      a3=el*(e3*px-el*pz)-e2*(e2*pz-e3*py)
      ak = sqrt(al**2+a2**2+a3**2)
      ell=al/ak
      el2=a2/ak
      el3=a3/ak
      thets=acos(el3)
      if(el3.lt.0.0) thets=acos(el3)+3.1416
      alfs=atan2(el2,ell)
      av=tan(.5*thets)
      xs=av*cos(alfs)
      ys=av*sin(alfs)
5     thet=theta/rad
      alf=alfa/rad
      write(30,3) x,y,xs,ys,thet,alf,sigs,sign,tau
      if (tau .ge. 0.0) then
      write(31,4) x,y
      write(32,4) xs,ys
      end if
      alfa=alfa+ainc*rad
      if(alfa.le.afin*rad) go to 2
      theta=theta+tinc*rad
      if(theta.le.tfin*rad) go to 1
3     format(9f8.3)
4     format(2f9.5)
6     format(1x,' SX=',f5.2,' SY=',f5.2,' SZ='
     & ,f5.2,' MU=',f5.2)
      close(31)
      close(32)
      stop
      end
```